JOURNAL OF AIRCRAFT
Vol. 46, No. 6, November–December 2009

Discrete Sweeping Jets as Tools for Improving the Performance of the V-22

Roman Seele,*,§ Philipp Tewes,*,§ and René Woszidlo*,§
University of Arizona, Tucson, Arizona 85721
Michael A. McVeigh†
The Boeing Company, Philadelphia, Pennsylvania 19142
and
Nathaniel J. Lucas* and Israel J. Wygnanski‡
University of Arizona, Tucson, Arizona 85721

DOI: 10.2514/1.43663

Experiments aimed at delaying flow separation through discrete jets pointing in the direction of streaming and sweeping side to side along the span were conducted on a V-22 airfoil with and without deflected trailing-edge flaps. The results indicated substantial drag reduction and lift increase at moderately low inputs of mass and momentum. Additional experiments were carried out on a semispan V-22 wing/nacelle combination, and they too provided an increase in lift-to-drag ratio L/D of approximately 60% (although active flow control was applied to the wing only). The effectiveness of the sweeping jets on reducing the download force acting on a V-22 full-span powered model in hover was also examined. A 29% reduction in download was realized using the embedded sweeping jets, corresponding approximately to a 2000 lb increase in hover lift.

Nomenclature

A_{slot}	=	total area of the nozzle exits
A_{wing}	=	area of the wing
C_{dt}	=	total drag coefficient
C_l	=	lift coefficient
C_μ	=	momentum coefficient
c_{flap}	=	flap chord length
D_L/F	=	download force-to-thrust force ratio
d_f	=	flap deflection angle
F	=	thrust force
J	=	jet momentum
L/D	=	lift-to-drag ratio
Re	=	Reynolds number
r	=	air density
U_{jet}	=	jet velocity
U_∞	=	freestream velocity
α	=	angle of attack

I. Introduction

THE modern tiltrotor aircraft combines the hover capability of the helicopter with the high-speed cruise capability of the fixed-wing aircraft. However, in hover, the wings experience a vertical drag or download from the impinging rotor downwash that reduces the achievable takeoff weight by approximately 15%. This is reduced to about 10% by deflecting the flap to a high angle to minimize the exposed area and vertical drag. Once a critical flap angle is exceeded, the download begins to increase because the flow over the flap separates. Using active flow control, the flow separation can be delayed and the download reduced further. In addition, the tiltrotor wing airfoil is usually thicker than a typical fixed-wing airplane and is prone to early separation with a consequent increase in drag. Using active flow control, this separation should be able to be delayed, thereby improving airplane cruise efficiency. This paper describes experiments to address these objectives through a series of tests on scale models, using active flow control from discrete sweeping jets rather than two-dimensional (2-D) omnidirectional pulsed jets.

Feedback-controlled sweeping jets were discovered at Harry Diamond Research Laboratories in Maryland more than 50 years ago. They are mostly used as sensors and fluidic amplifiers. However, they can generate adequate flux or force to be used as controllers or actuators. The sweeping character of the flow is achieved without the use of moving parts by incorporating a fluidic feedback loop into the nozzle design. The nozzle thrust is not hampered by the oscillations and its efficiency approaches 90% [1]. Viets [1], who tried to augment the effectiveness of ejectors, claims to have achieved hypermixing by increasing the mean spreading rates of the jet by a factor of 3 or more. Srinivas et al. [2], who analyzed a very large low-speed version of such a device (Fig. 1), were able to change its geometry (area ratios and divergence angle) as well as the jet exit velocity. They determined the effect of these parameters on the frequency and amplitude of the jet oscillation and concluded that the sweeping jet entrains less ambient fluid than its steady counterpart, in spite of the fact that its mean width might be an order of magnitude larger. The purpose of the present paper is to demonstrate that, even though the seemingly conflicting observations of Viets [1] and Srinivas et al. [2] are not resolved, these devices are very useful for active separation and circulation control.

The fluidic actuators used in the present investigation are similar to those shown schematically in Fig. 1. They are small and are driven by a high-pressure air source that enables the jet to oscillate at large angles relative to the axis of the nozzle and at a high frequency.

The following describes the experiments conducted on a V-22 airfoil and wing and on a complete one-10th-scale full-span powered model of the V-22 airplane in hover [3]. Fluidic actuation, originating from discrete nozzles distributed evenly along the span of the airfoil or the wing, is introduced over the flaps in all the configurations considered, in order to maintain flow attachment over the surface, reduce the drag or the download force, and increase the lift.

Presented as Paper 3868 at the 4th AIAA Flow Control Conference, Seattle, WA, 23–26 June 2008; received 5 February 2009; revision received 18 August 2009; accepted for publication 31 August 2009.

*Research Associate, Aerospace and Mechanical Engineering Department.
†Senior Technical Fellow.
‡Professor, Aerospace and Mechanical Engineering Department. Fellow AIAA.
§Please note that the sequence of the first three authors was chosen alphabetically.

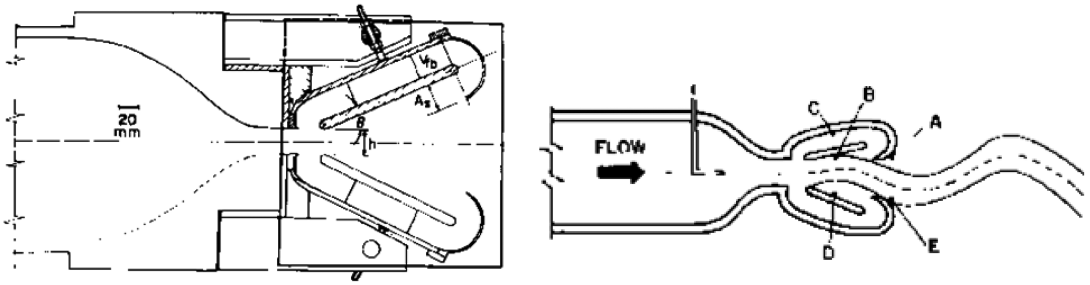

Fig. 1 Schematic drawing of sweeping jets [2].

II. Experimental Setup and Instrumentation

A. Two-Dimensional Tests

The 10.4 in. chord V-22 airfoil was tested in a cascade wind tunnel having a test section 24 in. high and 40 in. wide. The airfoil was mounted vertically, with its end plates embedded in the test section floor and ceiling, and thus its span was equal to the height of the test section (Fig. 2a). Approximately two chord lengths downstream of the airfoil trailing edge, a horizontal rake equipped with 16 total pressure tubes and two static pressure tubes at the rake edges was placed parallel to the freestream at the center of the test section (Fig. 2a). The space between adjacent pitot tubes was 1 in., requiring the rake to be traversed in order to provide the appropriate resolution of the wake data.

The 10.4%-scale V-22 main wing airfoil was made out of aluminum on a computer numerical control machine, and its flap was manufactured by stereo lithography. Two perforated brass tubes were connected to a high-pressure air system that supplied the compressed air needed by the actuators. The actuators were machined out of aluminum and inserted into the flaps, as shown schematically in Fig. 3. The flap on the V-22 had a Fowler motion and a flap seal or follower [a hinged flat surface joining the upper surface of the main airfoil to the upper surface of the flap (Fig. 3)]. During airplane flight with flaps retracted, this seal was closed, but it opened when the flap was deflected to allow flow from the lower surface through the gap to the upper surface of the flap. In hover, the gap was closed. The airfoil had scaled vortex generators (VGs) set at 20 deg to the freestream direction and placed at the appropriate locations on the model. Pressure distributions around the V-22 airfoil and velocity distributions in its wake were measured with a Pressure Systems, Inc. (PSI) 8400 system, using a LabVIEW [4] program to process the data. The accuracy of the PSI system is listed with $\pm 0.08\%$ of the full range of 2.5 kPa, which corresponds to an absolute error of ± 2 Pa. This value was never exceeded during the calibration procedure. To further improve the quality of the data, the LabVIEW program acquired pressure data repeatedly until a convergence criterion of 2% for the relative error of every port was satisfied.

B. Wing/Nacelle Semispan Model

The wing/nacelle semispan model was the same V-22 2-D airfoil model to which a wing-root box was added to hold the wing at a forward sweep of 6 deg and a dihedral angle of 3.5 deg. A flow-through nacelle (Fig. 2b) was also added. The wing VGs were placed to give a VG angle of attack of 20 deg, accounting for the wing forward sweep angle. The boundary layer generated over the nacelle was tripped at a location 2 in. aft of the front of the spinner. A No. 60 grit trip strip was also located inside the nacelle's inlet. Force measurements on the semispan wing were conducted in the University of Arizona's low-speed in-draft wind tunnel, which has a test section that is 48 in. wide and 34 in. tall. The test section operates at subatmospheric pressure because the flow is driven by a fan located at the end of the tunnel's diffuser. The tunnel is outfitted with a six-component table balance, which has a maximum error of 1%. For every instance, data were acquired for 20 s with a sampling rate of 1 kHz. All the experiments on the semispan V-22 wing were conducted at a freestream velocity of 25 m/s, providing a chord Reynolds number of $0.45 \cdot 10^6$.

C. Full-Span Powered Model

Download measurements were made on a powered 10.4%-scale V-22 airframe model that was suspended upside down from an A-frame located in a high-bay laboratory in order to avoid ground

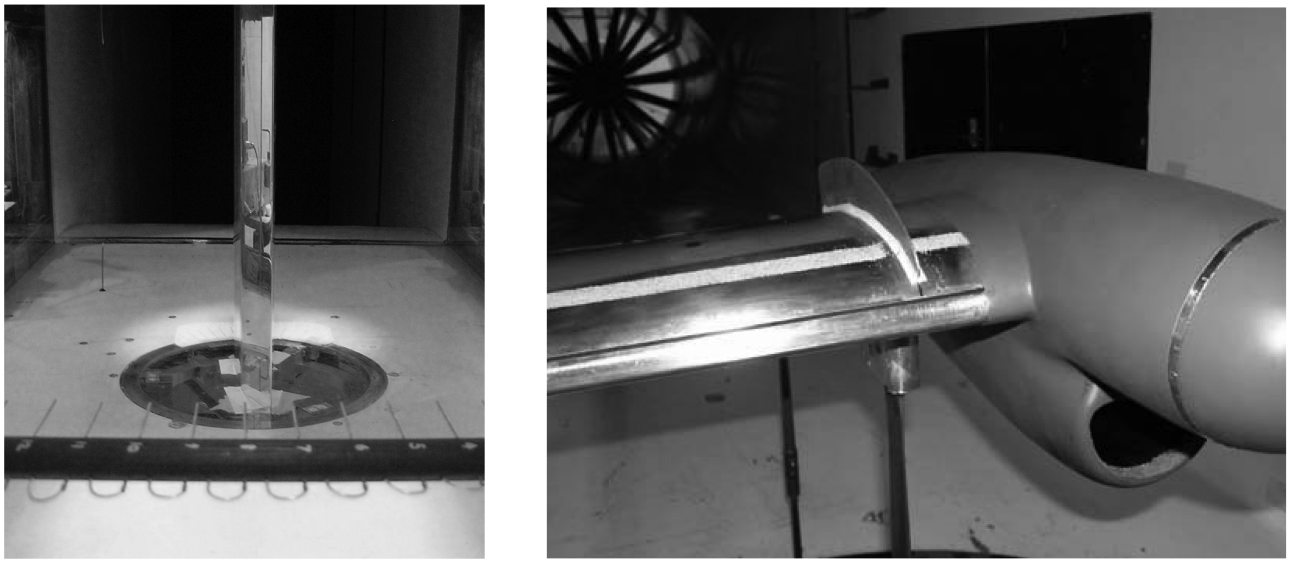

a) b)

Fig. 2 Installation of V-22 wing/nacelle combination and airfoil in respective wind tunnels.

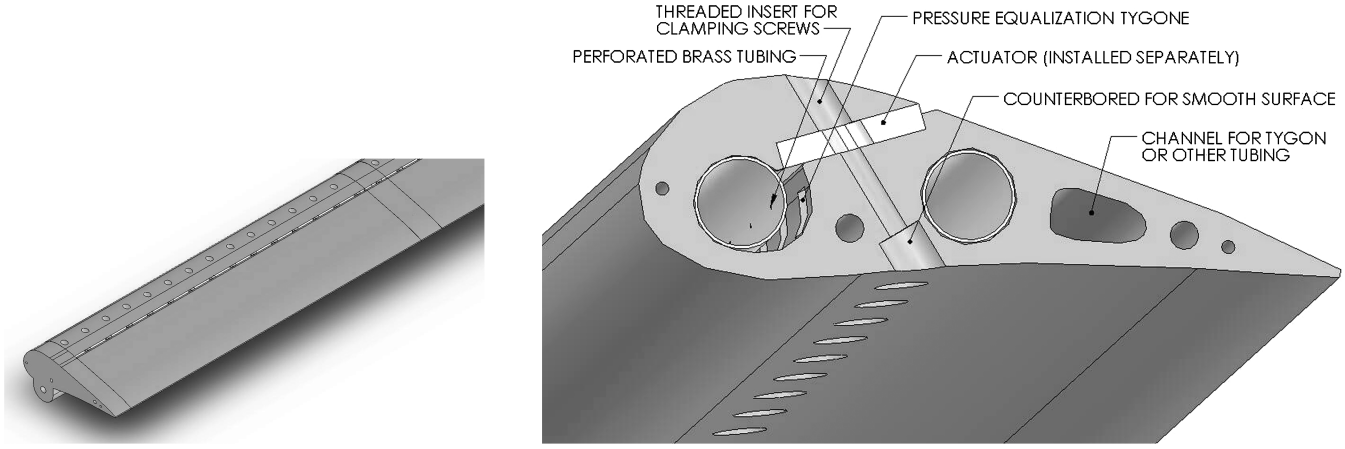

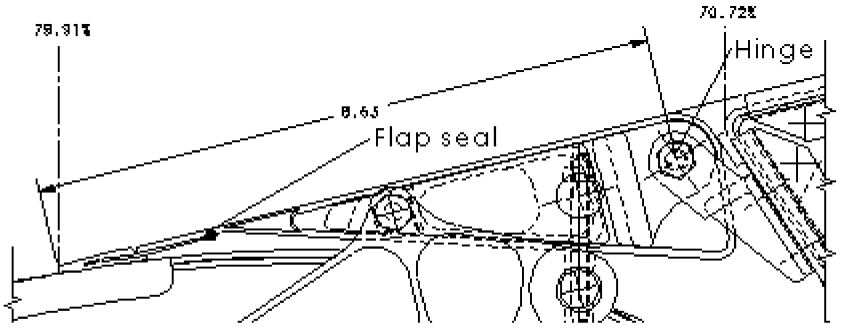

Fig. 3 V-22: a) the flap, b) installation of the actuators, and c) flap-seal arrangement.

effects (Fig. 4). The two scaled 4-ft-diam three-bladed counter-rotating rotors were mounted on stacks bolted to the laboratory floor. The rotors were not connected to the airframe model in order to separate rotor forces from the airframe forces associated with the impingement of the rotor flow on the model. The gap between the rotors and the model's nacelles was approximately 1 in.. The collective pitch of both rotors was set to give a thrust coefficient of 0.016, and the rotational speed was maintained at 2200 revolutions per minute (RPM). For the initial evaluation of the rotors, the wake downwash velocities were measured in the absence of the model using a pitot-static probe that was traversed in the radial direction at distances below the rotors, corresponding approximately to the absent wing. The data were used to calculate the momentum coefficient of the actuators. The thrust of each rotor was measured directly by a balance in each stack, and torque was measured by transducers on the transmission shafts.

The A-frame support structure was 9 ft tall, and the model's fuselage base was typically 18 in. below the support structure. The model incorporated a wing with adjustable flaps. The wing was hollow and made of aluminum; the flaps were made using stereo lithography. The fuselage was made of plywood ribs covered with foam. An internal metal structure supported the wings. Most

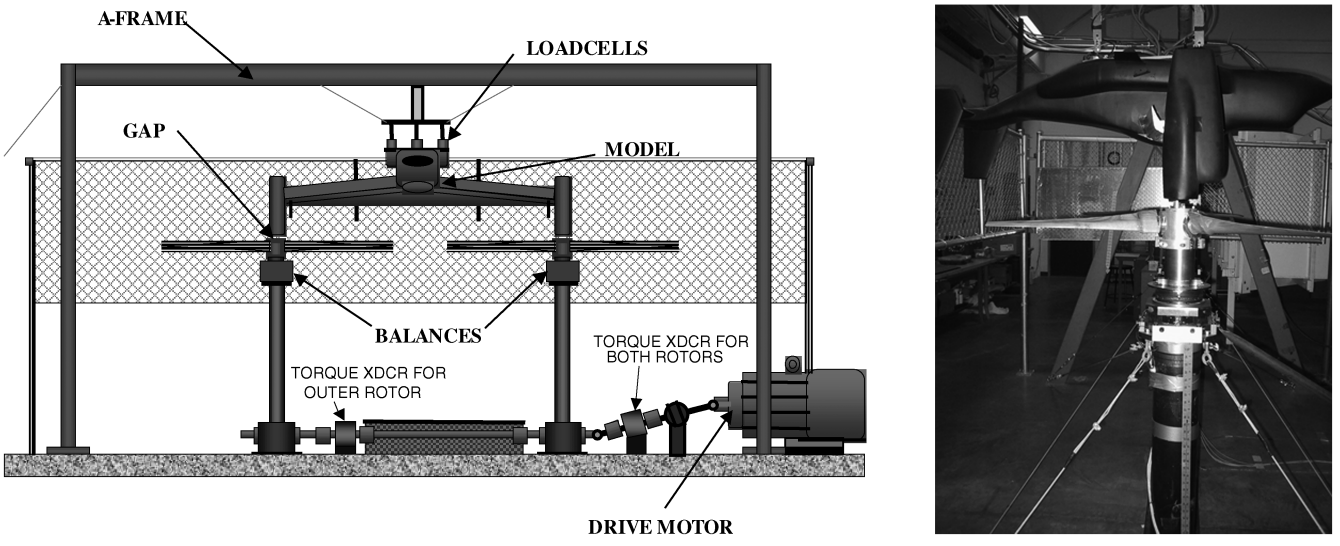

Fig. 4 Schematic diagram and picture of the download rig. (XDCR denotes transducer).

plumbing was routed through the wings and fuselage to maintain an open flowfield and avoid protuberances on the model. The bottom surface of the fuselage had hard points built in to attach to a half-inch aluminum plate. A tripod fixture suspended from the A-frame was attached to this plate by three Interface Model 1500 load cells, which enabled force measurements with an accuracy of 0.05% full scale. Because the rotors were not coupled to the model, the load cells could directly measure the total aerodynamic download force on the model. The load cells were arranged in a T configuration to provide the vertical load and rolling and pitching moments. The rotors were exact scale replicas of the V-22 rotor blades, including twist, planform, and airfoil sections. A 40 HP electric, frequency controlled, variable RPM motor powered the rotors. The maximum recommended operating speed of rotation was 2400 RPM and was controlled via a remote panel wired to the motor controller.

The fluidic actuators were similar in concept to the designs in [5] and were distributed over the entire span of the flap on the V-22 airfoil (Fig. 3). The distance between adjacent nozzles was arbitrarily selected to be 0.75 in., but experiments were also carried out with every other exit nozzle blocked off. The voids in the V-22 flap, acting ideally as accumulators, were pressurized to force air through the actuators. A silicone gasket sealant was used on the surfaces abutting the actuators to prevent air leakage. The volume flow of air was measured with a flow meter at the inlet to the flap during a calibration procedure and was corrected for the pressure at that location. There was a large pressure drop between the flow meter and the throat of the nozzles, for which the square area was less than 0.003 in.^{2}. Thus, the pressure at the throat was unknown. The jet exit velocity was therefore calculated assuming continuity and neglecting compressibility at the nozzle exit (i.e., $U_{\text{jet}} \cdot A_{\text{slot}} = \text{const}$, where the area A_{slot} refers to the total area of all exit nozzles). The jet velocity was used to calculate the momentum coefficient C_μ, defined by

$$C_\mu = 2\frac{A_{\text{slot}}}{A_{\text{wing}}}\left(\frac{U_{\text{jet}}}{U_\infty}\right)^2 = \frac{J}{1/2\rho U_\infty^2 A_{\text{wing}}} \tag{1}$$

where $J = \rho U_{\text{jet}}^2 A_{\text{slot}}$ is the jet momentum.

Because this formula did not account for the angular sweeps of the jets, its validity was checked by mounting the V-22 flap on a knife edge and measuring the thrust force F generated by the sweeping jets. The value of F/J is plotted in Fig. 5. For the densely distributed actuators spaced 0.75 in. apart and at a calculated $U_{\text{jet}} = 50$ m/s, the agreement between calculated and measured thrust was excellent. However, agreement between the two methods decreased as U_{jet} increased. A major reason for this might be that the jet oscillated more to the sides as the pressure increased, thus reducing the thrust in the x direction. This was reinforced by the observation that doubling the distance between actuators reduced the ratio of F/J because the jets were able to oscillate at larger amplitudes before colliding and interfering with their neighbors. Compressibility and flow separation within the actuator's body might also contribute to the decreasing values of F/J. The frequency of the jet oscillations was measured with a hot-wire probe placed close to the jet exit. The applied flow rates resulted in frequencies of the order of 1 kHz.

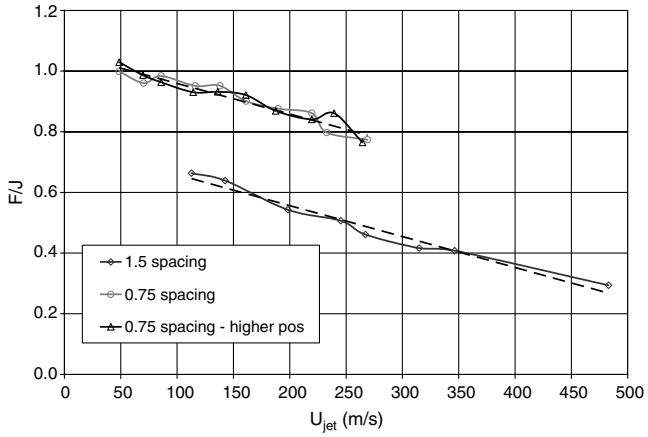

Fig. 5 Ratio of measured to calculated jet thrust as a function of calculated jet velocity.

III. Results

A. V-22 Airfoil

Tests were conducted on the V-22 airfoil using the actuation arrangement shown in Fig. 3. The data were acquired at $Re=$ 360, 000, and the airfoil had scaled VGs located on its upper surface near the leading edge. A roughness strip was placed on the airfoil's lower surface at 35% chord to ensure tripped flow. The first set of data was taken at zero flap deflection. In this case, the flap seal was firmly attached to the flap surface, preventing any flow through the cove (essentially making this configuration a single-element cambered airfoil). The actuators were located just downstream of the flap follower. The data shown in Fig. 6 correspond to a spanwise actuator spacing of 0.75 in..

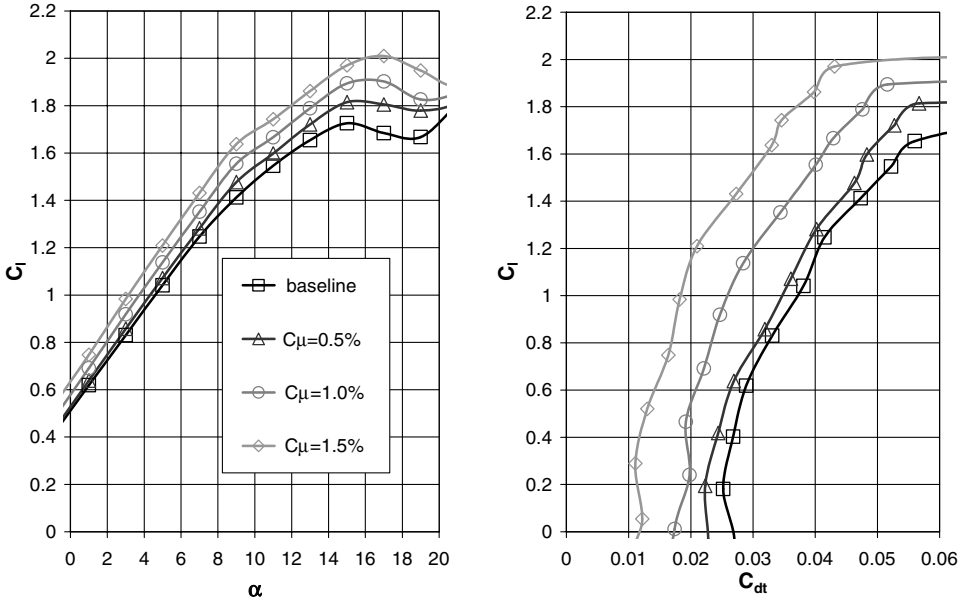

Fig. 6 Lift and drag characteristics of the V-22 airfoil ($Re = 360, 000$, $\delta_f = 0$ deg) actuation at 30% flap chord.

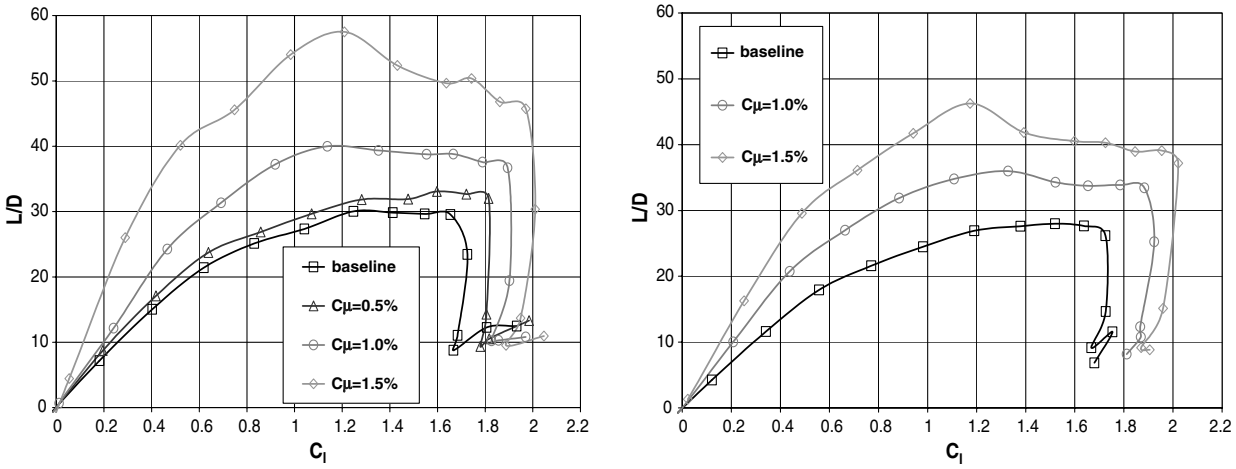

Fig. 7 V-22 airfoil L/D at $Re = 360,000$ ($\delta_f = 0$ deg) actuation at 30% flap chord: a) flap follower sealed to flap and b) 0.02 in. gap between the flap follower and the flap.

Fluidic actuation increased the lift and decreased the drag of this airfoil at all angles of attack, possibly because the V-22 airfoil is aft loaded and the flow might not be fully attached, even when the VGs are present. At angles of attack $\alpha > 6$ deg, $dC_l/d\alpha$ of the basic airfoil was reduced, pointing to a possible separation or at least a thick boundary layer. Fluidic actuation at $C_\mu = 1.5\%$ halved the drag around $C_l = 1$ (Fig. 6) and doubled the L/D in that range of C_l (Fig. 7). The actuators in this experiment were inclined at 30 deg to the surface of the flap (Fig. 3), as this angle gave good results when periodic actuators were used. The significance of this inclination angle was never properly investigated in either application, and it would have to be determined in order to optimize the system. As a consequence of the actuation at $C_\mu = 1.5\%$, the maximum lift-to-drag ratio $(L/D)_{\max}$ increased from 29.7 for the baseline to 57.5, provided the gap between the flap follower and flap was sealed (Fig. 7a). A gap of 0.02 in. reduced the effectiveness of the actuation, yielding an $(L/D)_{\max}$ of 46 for the same C_μ. One might conclude that suction through the gap was disruptive, but it is also possible that the jets were being squeezed between the flap surface and the follower.

Lowering the flap to 20 deg (Fig. 8) increased $C_{l\max}$ of the baseline airfoil from 1.7 (measured at $\delta_f = 0$ deg) to 2.45 and almost doubled the drag at lift coefficients around $C_l = 1$. Lowering the flap also created a gap of 0.061 in. between the bottom of the flap follower and the flap's upper surface, allowing air to pass from the airfoil lower surface to the upper surface. Actuation with $C_\mu = 2\%$ increased C_l at small values of α by $\Delta C_l = 0.6$, but the increase in $C_{l\max}$ was only 0.2. The reduction in drag due to the sweeping jets around $C_l = 1.5$ was approximately $\Delta C_{\mathrm{dt}} = 0.04$, an approximately 50% decrease. Although these results were measured at a low Reynolds number, they may indicate potential improvements at flight Reynolds numbers. Reduced drag at high C_l would be valuable for a flaps-deflected conventional landing approach. For loitering, which occurred at a lower C_l, the data suggested that it was more effective to loiter with the flaps up and using fluidic actuation on the undeflected flap, generating $L/D = 57$ at $C_l = 1.2$, rather than on the deflected flap, that generated L/D of only 40 for the same lift coefficient, the same C_μ of 1.5%, and the same actuation location (Figs. 7a and 9a).

Moving the actuators 0.3 in. upstream to 20% flap chord had a major effect on the results at the higher levels of momentum input (Fig. 9b). In this position, the sweeping jets emanated from beneath the flap follower and might either act as ejectors or block the flow through the flap cove. The latter assumption seemed more plausible in view of the deterioration of actuation performance whenever the gap was open. Nevertheless, the jets were forced to be close to the

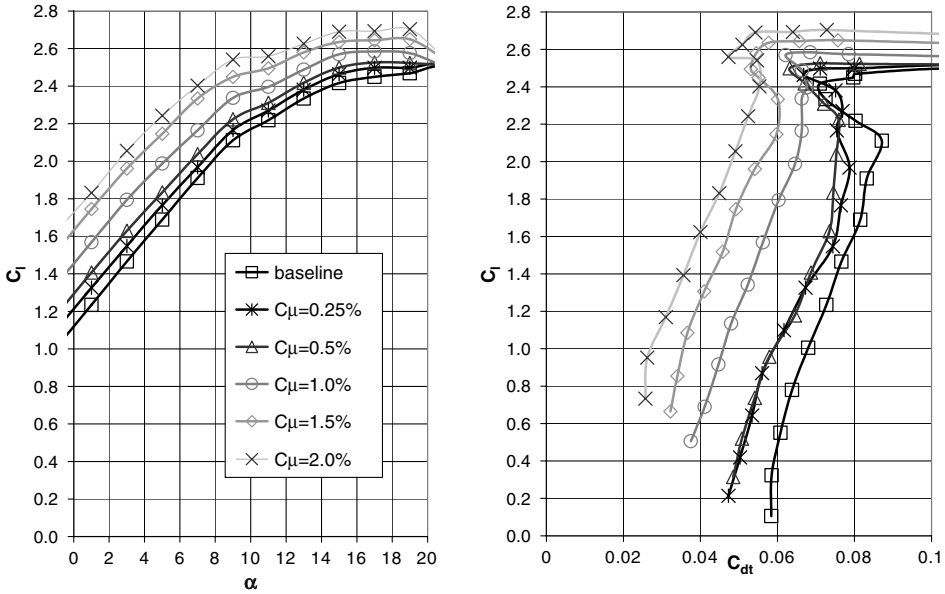

Fig. 8 Lift and drag of V-22 airfoil ($Re = 360,000$, $\delta_f = 20$ deg) actuation at 30% flap chord with a flap-seal gap of 0.061 in..

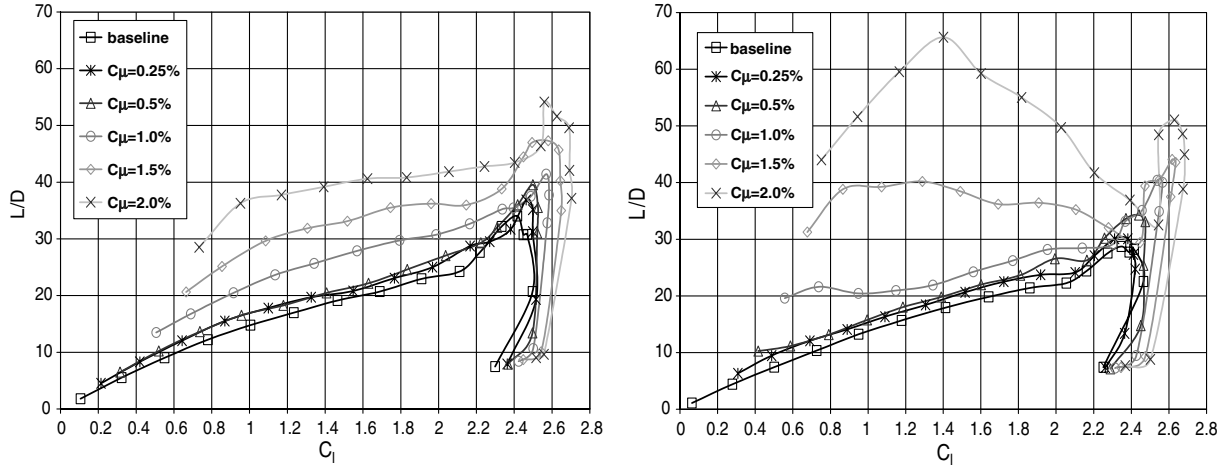

Fig. 9 Actuator location effect on L/D for V-22 airfoil ($Re = 360,000$, $\delta_f = 20$ deg) with actuator spacing of 0.75 in. and a follower gap of 0.061 in.: a) actuation at 30% flap chord and b) actuation at 20% flap chord.

surface by the follower and they increased the L/D from 40 to 65 when $C_\mu = 2\%$. The increases in L/D only occurred above a threshold of $C_\mu > 0.5\%$ (Fig. 9). The preceding results indicated that airplane power required for level flight could be substantially reduced using sweeping jet actuation.

Because the actuator array was machined out of a solid strip of aluminum, the distance between adjacent actuators was arbitrary and bore no relationship to wing or flap chord. Such a relationship should be explored in future research. To assess the effect of spanwise spacing of the actuators, the distance between adjacent actuators (i.e., actuator spacing) was doubled by blocking every second actuator in the array. A sample of the results is shown in Fig. 10, in which the results in Fig. 10a are comparable with the airfoil results in Fig. 7a, and those in Fig. 10b are compared with Fig. 9b. It is clear that doubling the distance between adjacent actuators decreased the effectiveness of the actuation when all other parameters, including the average C_μ, remained constant. The maximum L/D corresponding to $C_\mu = 1.5\%$ was reduced from 57 (Fig. 7a) to 41 (Fig. 10a) at $\delta_f = 0$ deg. When $\delta_f = 20$ deg (Fig. 9b and 10b) and there was a gap between the flap seal and the flap, the increase in the actuator spacing not only lowered the maximum L/D from 40 to 30 at $C_\mu = 1.5\%$ and from 65 to 35 at $C_\mu = 2\%$, but the lift at which the maximum occurred also dropped from $C_l = 1.4$ to $C_l \approx 0.9$. In both cases, $C_\mu < 1\%$ had no effect on L/D.

B. V-22 Semispan Wing/Nacelle Model

A six-component balance was used to determine the forces and moments acting on the V-22 wing/nacelle model (Fig. 2). The thrust of the jet used in calculating C_μ could therefore be obtained in situ in absence of the wind. The thrust was in good agreement with the results of the calibration of the sweeping jets. The results, presented as a normalized L/D ratio versus a normalized lift coefficient, showed improvements due to the use of sweeping jets.

Even though $C_{L\max}$ for the finite wing was reduced by aspect ratio effects, the lift characteristics at $\delta_f = 0$ deg were quite similar to the 2-D results, shown in Fig. 7. The drag, however, was substantially higher because of the nacelle and the induced drag on this aspect ratio 5 wing. Figure 11a indicates that for $C_\mu = 2\%$, a 60% improvement in L/D was realized at approximately the same lift coefficient at which the baseline wing attained its best performance. Much of this performance gain disappeared when the spacing between adjacent actuators was doubled (Fig. 11b). With the larger actuator spacing, there was no improvement in L/D at values of $C_l < 0.7$, suggesting the absence of separation at these low values of angle of attack.

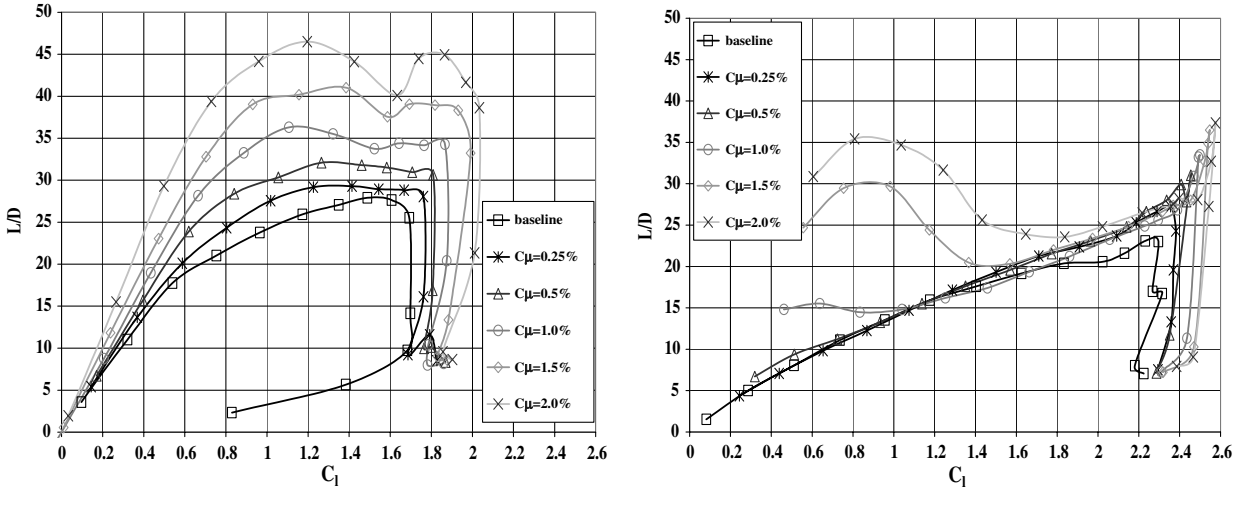

Fig. 10 Effect on L/D of 1.5 in. actuator spacing on V-22 airfoil ($Re = 360,000$): a) $\delta_f = 0$ deg with no gap and actuation at 30% flap chord, and b) $\delta_f = 20$ deg, with the gap = 0.061 in. and the actuation at 20% flap chord.

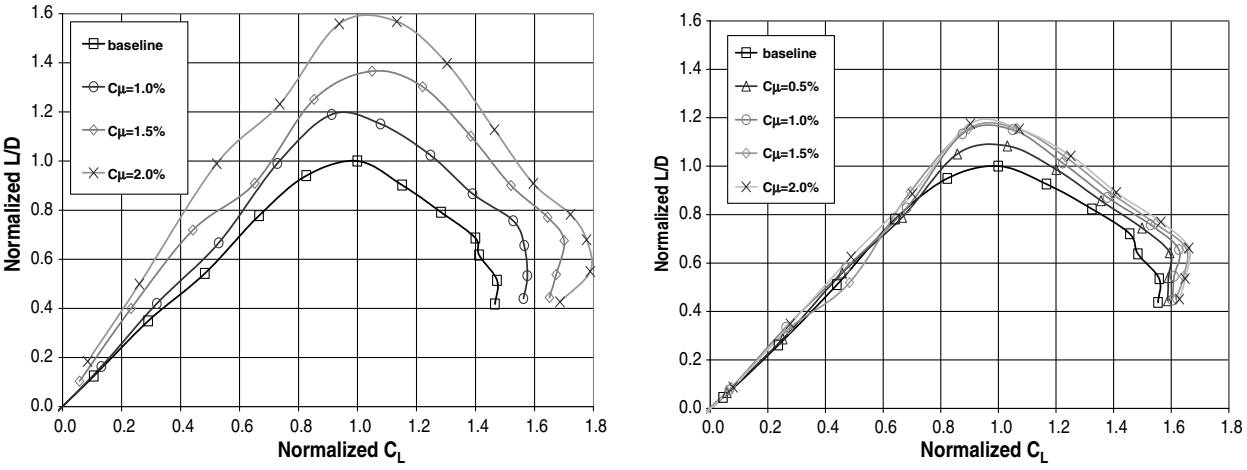

a) b)

Fig. 11 Normalized L/D of V-22 wing/nacelle ($Re = 450,000$, $\delta_f = 0$ deg) actuation at 30% flap chord with the gap sealed: a) 0.75 in. actuator spacing and b) 1.5 in. actuator spacing.

$(L/D)_{\max}$ was increased by 20% for $C_\mu = 1\%$. An increase to $C_\mu = 2\%$ did not produce additional improvement.

Deflecting the flap to $\delta_f = 20$ deg, with the accompanying gap of 0.061 in. between the flap follower and the upper surface of the flap, reduced the effectiveness of the sweeping jets (Fig. 12). The improvement in L/D for actuators located at 30% of the flap chord was only 10% (Fig. 12a) in comparison to over 100% improvement in the 2-D airfoil's L/D under similar conditions (Fig. 9a). Moving the actuator location on the flap upstream to 20% flap chord (Fig. 12b) increased $(L/D)_{\max}$ by 20%. The effectiveness of the sweeping jets on the finite wing was reduced compared with the 2-D results, partly because of the induced drag C_{Di} which is proportional to C_L^2. The adverse effect of the gap between the flap and the flap follower on the finite wing was also noted (Fig. 12a vs Fig. 11a), as well as the improvement realized by moving the actuation location upstream (Fig. 12b).

C. Hover Download on the V-22 One-10th-Scale Powered Model

The variation of the normalized download-to-thrust ratio of the V-22 model in hover with flap deflection is presented in Fig. 13. The top curve (solid squares) was the download without actuation. The value for the minimum download and the value of the flap deflection at which it occurs were used to normalize the data. Two C_μ values were listed: the one on the left was obtained from the measured mass flow, and the one on the right used the calibrated thrust, shown in Fig. 5. In this case, the discrepancy between the momentum coefficients based on the calculated mass flow passing through the measured nozzle area and those based on the calibrated thrust was small (e.g., $(C_\mu)_{\text{flow}} = 2.76\%$ vs $(C_\mu)_{\text{thrust}} = 2.24\%$). This difference was attributed in part to the spanwise excursions of the sweeping jets that result in a reduction of the streamwise component of thrust. When the gap between adjacent nozzles was increased to 1.5 in. there was a substantial reduction in thrust (Fig. 5) because the reduced interference between adjacent jets allowed larger amplitude sweeping, enclosing a ± 60 deg angle relative to the thrust vector. In this case, the assumption that the entire jet momentum appeared as thrust failed. According to the manufacturer of the actuators, there was no phase correlation between adjacent jets and, therefore, the interference and realignment in the direction of streaming depended directly on the distance between them.

As C_μ was increased, the optimal flap deflection for minimum download increased as the fluidic actuation was able to keep the flow attached to higher flap angles. The maximum download alleviation attained using the sweeping jet fluidic actuators was 29%. This was achieved when the space between adjacent actuators was 0.75 in. and they were located at 20% flap chord; flap deflection angle was increased by as much as 28%. This download alleviation trend

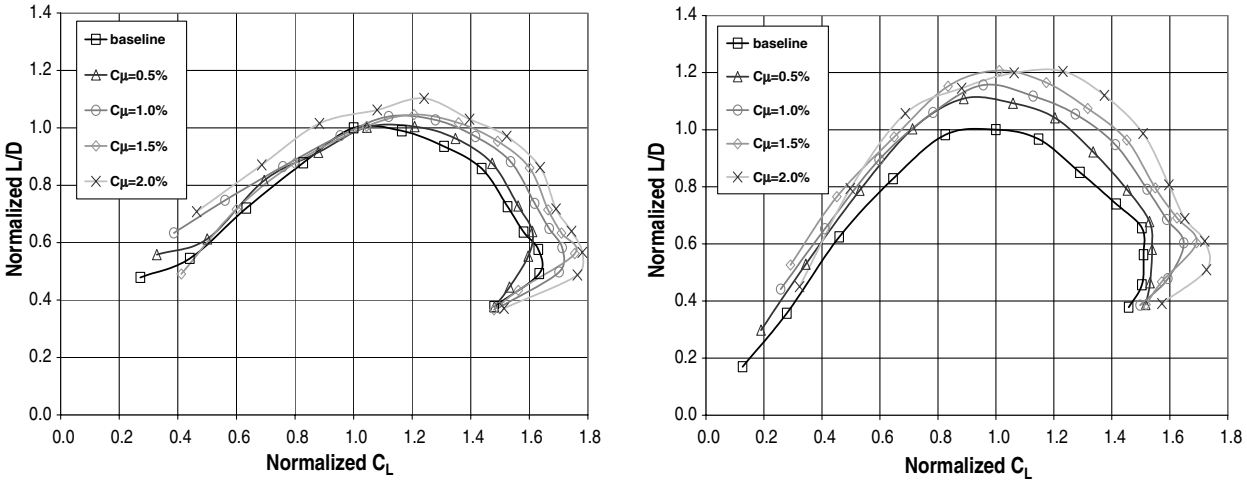

a) b)

Fig. 12 Normalized L/D of V-22 wing ($Re = 450,000$, $\delta_f = 20$ deg) with the gap = 0.061 in. and 0.75 in. actuator spacing: a) actuation at 30% flap chord and b) actuation at 20% flap chord.

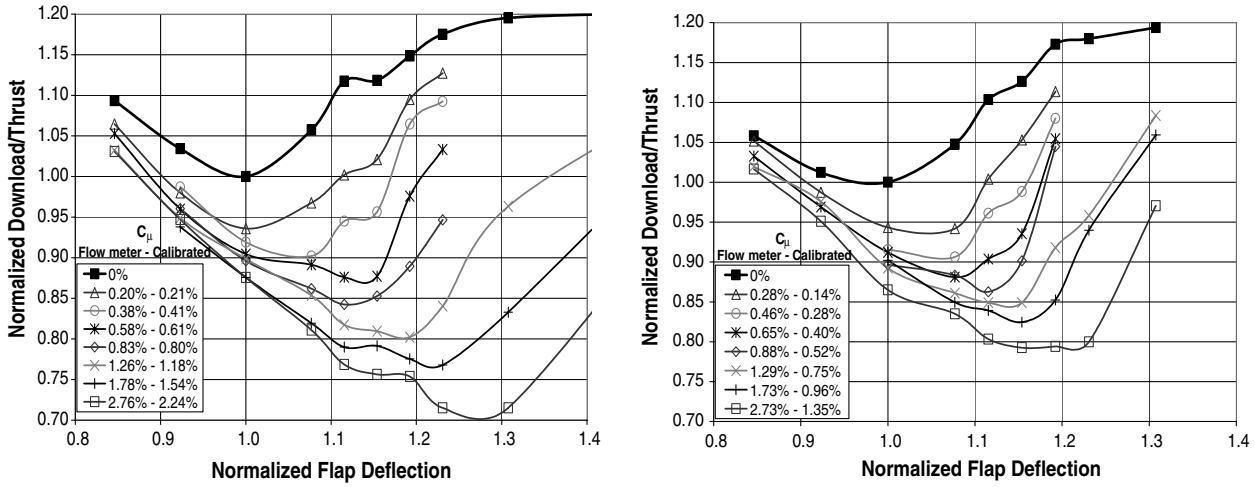

Fig. 13 Normalized hover download-to-thrust ratio vs flap deflection with actuation at 20% flap chord: a) 0.75 in. actuator spacing and b) 1.5 in. actuator spacing.

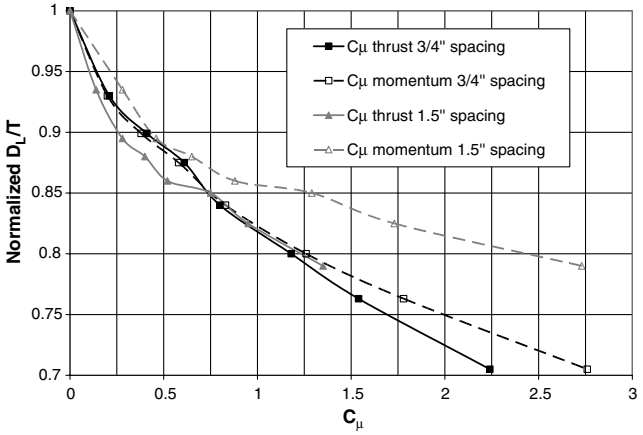

Fig. 14 Normalized minimum values of D_L/T vs C_μ obtained from thrust or momentum.

compared very favorably with previous results generated by pulsed jets from electromagnetic actuators, although those reduced the download by only 17%.

The spanwise distance between adjacent actuators was increased to 1.5 in., and the resulting variation of download-to-thrust ratio D_L/T with C_μ and flap deflection was plotted in Fig. 13b. The two sets of results trended well with the C_μ calculated from the measured thrust but less so with the C_μ based on calculated mass flux (Fig. 14). To attain the largest download alleviation at minimum mass flow, the optimal distance between the actuators and their location on the flap would have to be established by future testing.

It would be desirable to have a single location for the actuators that would provide the largest download reduction in hover as well as increases in airplane L/D. This might be possible by either installing the actuators inside the flap at $x/c_{\text{flap}} > 30\%$ or installing them in the flap follower. The latter could not be easily simulated on the one-10th-scale model. However, moving the actuator location downstream to 30% of the flap chord was evaluated. The resulting download measured at identical conditions to those shown in Fig. 13a was plotted in Fig. 15 for actuators located at 30% flap chord. A deterioration of only 3% in the download alleviation resulted, suggesting that a single position might be feasible.

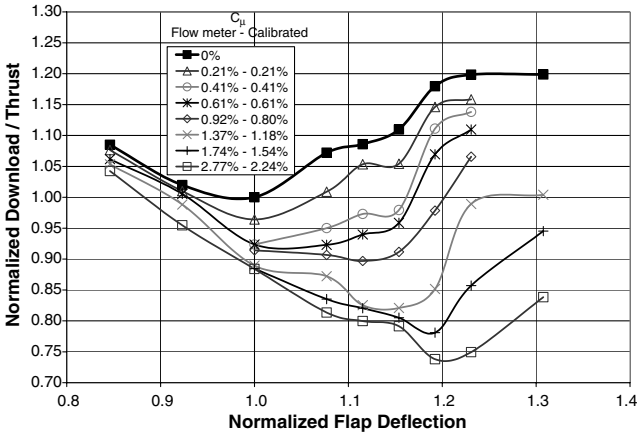

Fig. 15 Dependence of normalized download-to-thrust ratio in hover on C_μ and on flap deflection, with actuation at 30% flap chord and 0.75 in. actuator spacing.

IV. Conclusions

A spanwise line of discrete jets pointing in the flow direction and sweeping spanwise has been demonstrated to provide effective flow control on a V-22 airfoil and a semispan V-22 wing/nacelle combination. Because a typical distance from actuation to the trailing edge of an airfoil is almost two orders of magnitude larger than the dimension of the nozzle, and because in an axisymmetric jet the maximum jet velocity is inversely proportional to the distance from the nozzle, one expects the jet velocity to become comparable with U_∞ far upstream of the trailing edge of the airfoil. If this is the case, it appears that the sweeping jets delay flow separation by acting more like VGs that enhance mixing with the external flow than as jets that energize the boundary layer. This was perhaps the reason that, in the absence of separation (e.g., on the thinner NACA 0015 airfoil with $\delta_f = 0$ deg [6]), this type of fluidic actuation was totally ineffective yet was effective on a thicker V-22 airfoil. One might conclude that separated flow is required for the sweeping jets to be useful.

The results on the V-22 semispan finite wing/nacelle model showed substantial drag reduction and lift enhancement that increased the wing/nacelle L/D by 60%. The sweeping jets also permitted large flap deflections in hover without separation, thus reducing the download force on a powered tiltrotor model by almost 30%. If implemented on the actual aircraft, these actuators would permit a higher takeoff weight while substantially improving loiter efficiency. These results were achieved without optimization of the actuator spacing, its dimensions, or its location. The improvements were also achieved without a full understanding of the manner in which the actuators interacted with the separated flow. More research

is necessary in order to further improve the effectiveness and understanding of this type of actuation.

Acknowledgments

This project was funded by the Center for Rotorcraft Innovation (CRI) and the National Rotorcraft Technology Center (NRTC), the U.S. Army Aviation and Missile Research, Development, and Engineering Center (AMRDEC) under the Technology Investment Agreement W911W6-06-2-0002, entitled the National Rotorcraft Technology Center Research Program. The authors would like to acknowledge that this research and development was accomplished with the support and guidance of the NRTC and CRI. The views and conclusions contained in this document are those of the authors and should not be interpreted as representing the official policies, either expressed or implied, of the AMRDEC or the U.S. Government. The U.S. Government is authorized to reproduce and distribute reprints for Government purposes, notwithstanding any copyright notation thereon.

References

[1] Viets, H., "Flip-Flop Jet Nozzle," *AIAA Journal*, Vol. 13, No. 10, Oct. 1975, pp. 1375–1379. doi:10.2514/3.60550

[2] Srinivas, T., Vasudevan, B., and Prabhu, A., "Performance of Fluidically Controlled Oscillating Jet," *Proceedings of the IUTAM Symposium: Turbulence Management and Relaminarization*, A89-10154 01-34, Springer–Verlag, New York, 1988, pp. 485–494.

[3] Schmalzel, M., Varghese, P., and Wygnanski, I., "Download Alleviation on a V-22 Model Having a Simple Flap Used in Conjunction with Periodic Excitation, Suction, and Blowing," International Powered Lift Conference, Society of Automotive Engineers Paper 2005-01-3188, 2005.

[4] LabVIEW Software, Ver. 8.5, National Instruments.

[5] Gregory, J. W., Sullivan, J. P., Raman, G., and Raghu, S., "Characterization of a Micro Fluidic Oscillator for Flow Control," 2nd AIAA Flow Control Conference, AIAA Paper 2004-2692, June 2004.

[6] Zakharin, B., Woszidlo, R., and Wygnanski, I., "Some Recent Observations on Turbulent Mixing and Control of Separation that Focus on the Perseverance of Streamwise Vorticity," International Conference on Jets, Wakes, and Separated Flows (ICJWSF), Tech. Univ. of Berlin, Sept. 2008.